RSC Advances

PAPER

View Article Online
View Journal | View Issue

Cite this: *RSC Adv.*, 2020, **10**, 17129

Impact of ammonium sulfite-based sequential pretreatment combinations on two distinct saccharifications of wheat straw†

Guang Yu,[ab] Shiyue Liu,[ab] Xiaoyan Feng,[a] Yuedong Zhang,[a] Chao Liu,[a] Ya-Jun Liu,*[a] Bin Li,*[a] Qiu Cui[a] and Hui Peng*[a]

The properties of lignocellulosic substrates obtained from different pretreatments have a big impact on downstream saccharification based on both the fungal cellulase system and the cellulosome-based whole-cell biocatalysis system. However the corresponding effect of these two distinct saccharification strategies has not been comparatively analyzed. In this work, three ammonium sulfite (AS)-based pretreatment combinations (*i.e.*, AS + hydrothermal (HT) pretreatment, AS + xylanase (X) pretreatment, and HT + AS pretreatment) were conducted to treat wheat straw. The obtained pretreated substrates with different properties were saccharified using fungal cellulase or an engineered *Clostridium thermocellum* strain as the whole-cell biocatalyst, and the ability to release sugar was comparatively evaluated. It was found that for the whole-cell saccharification, the total sugar digestibility of AS + HT/X pretreated wheat straw was 10% higher than that of HT + AS pretreated wheat straw. However, for fungal cellulase-based saccharification, the enzymatic hydrolysis efficiency was less susceptible to the sequence of pretreatment combinations. Hence, the whole-cell biocatalysis system was more sensitive to substrate accessibility compared to the free enzymes. In addition, the characterization and analyses showed that AS + HT/X pretreatment could remove more lignin, generating a more accessible surface with a larger external surface and lower surface lignin coverage, compared to the HT + AS pretreatment. Therefore, the AS + HT/X pretreatment was more compatible with the cellulosome-based whole-cell saccharification.

Received 24th February 2020
Accepted 22nd April 2020

DOI: 10.1039/d0ra01759k

rsc.li/rsc-advances

1. Introduction

Agricultural straw is one of the most abundant lignocelluloses, and its annual production in China is over 600 million tons.[1] However, previously most of this was burned directly in the field, which caused serious environmental issues and waste of natural resources. Currently, the burning of agricultural waste is strictly forbidden, and simultaneously energy demand is increasing. Therefore, the Chinese government plans to use gasoline blended with 10% bioethanol for motors nationwide by 2020, which would require more than 10 million metric tons (about 3.3 billion gallons) of bioethanol.[2] Also, the US Energy Independence and Security Act requires 36 billion gallons of biofuel by 2022. Yet, currently, over 90% of bioethanol is produced from corn instead of lignocelluloses in the US and China.[3] In this case, the development of cellulosic ethanol by making better use of agricultural waste (*e.g.*, wheat straw) has become an urgent matter.

Cellulosic ethanol production usually includes feedstock collection, pretreatment, saccharification, fermentation, and purification processes. Among them, pretreatment as an essential step to deconstruct the natural recalcitrance of lignocellulosic matrix has great influence on the downstream saccharification.[4] It has been proved that high lignin content of lignocellulosic substrate could restrict the efficiency of enzymatic hydrolysis, because of the physical barrier of lignin and the nonproductive binding between cellulase and lignin.[5] Thus, rupturing lignocellulosic cell walls *via* lignin removal is one of the most commonly used strategies for biomass pretreatment, including biological (*e.g.*, white-rot fungi) methods,[6] alkali-based pretreatment (*e.g.*, dilute NaOH, aqueous ammonia),[7–9] sulfite pretreatment (*e.g.*, sulfite pretreatment to overcome recalcitrance of lignocellulose (SPORL) method),[10] and organic solvent pretreatment (*e.g.*, formic acid pretreatment).[11] Among these approaches, ammonium sulfite (AS) pretreatment can efficiently remove lignin of lignocellulose *via* ammonolysis and sulfonation of lignin, thus enhancing the accessibility of

[a]*CAS Key Laboratory of Biofuels, Shandong Provincial Key Laboratory of Synthetic Biology, Shandong Engineering Laboratory of Single Cell Oil, Qingdao Engineering Laboratory of Single Cell Oil, Dalian National Laboratory for Clean Energy, Qingdao Institute of Bioenergy and Bioprocess Technology Chinese Academy of Sciences, Qingdao, 266101, China. E-mail: libin@qibebt.ac.cn; liuyj@qibebt.ac.cn; penghui@qibebt.ac.cn*

[b]*University of Chinese Academy of Sciences, Beijing 100049, China*

† Electronic supplementary information (ESI) available. See DOI: 10.1039/d0ra01759k

cellulose.[12,13] Also, the spent liquor of AS pretreatment can be used to produce lignin-based fertilizer due to the high nitrogen contents,[14] and the sulfonated lignin can be used to produce other products as well, such as concrete water-reducer, dye dispersant, or surfactant,[7] to further improve the economic feasibility and sustainability of the entire process of AS pretreatment.

In addition, the presence of hemicellulose is also a barrier to cellulase, as reported previously.[15] Hydrothermal (HT) pretreatment (known as liquid hot water treatment or autohydrolysis) is an attractive and sustainable approach as well, because no chemical is added and just compressed hot water or steam is used in HT pretreatment. In HT process, acetyls of hemicelluloses are first released, generating a weak acid condition to further promote degradation of hemicelluloses into soluble oligomers and xylose.[16] Besides, xylanase treatment can release xylooligosaccharides, which is also a green approach for hemicelluloses degradation.[17] Hence, it is expected that by combining AS with HT/xylanase pretreatment, the efficiency of downstream saccharification could be highly improved and the main components of feedstock could be better utilized.

Except for pretreatment, the high cost of enzymatic saccharification (approximate 25–30% of the total cost) impedes the commercialization of cellulosic ethanol for a long period.[18] Free fungal cellulase is commonly used for cellulose hydrolysis to sugars at present. Although enzymatic hydrolysis already technically meets the requirements for the production of cellulosic ethanol, the cellulosic ethanol is still uncompetitive to the corn ethanol to a large extent due to the high cost of enzyme.[19] Besides the off-site saccharification employing free cellulase as the biocatalyst, on-site saccharification processes, including consolidated bioprocessing (CBP) and consolidated bio-saccharification (CBS), have been proposed to simplify the process and reduce the enzyme cost.[20] Unlike CBP technology which is mainly for the production of cellulosic ethanol by combining enzyme production, hydrolysis and fermentation steps in one reaction,[21] the CBS strategy separates fermentation from the integrated process and CBS determines fermentable sugars as the product for flexible downstream applications.[22] CBS mainly employs cellulosome-producing microorganisms as the whole-cell biocatalyst to convert cellulosic substrates to fermentable sugars. As a multi-protein supermolecular complex derived from anaerobic bacteria, the cellulosome outperforms commercial fungal cellulase cocktails in the degradation of pure cellulose, especially towards the crystalline region. *Clostridium thermocellum* is considered one of the most promising candidates as a whole-cell biocatalyst for CBS because of its highly efficient cellulosome and the themophilic growth condition.[23,24] The CBS technology is a newly proposed strategy which is being in the stage of lab scale. However, it has the advantage on cost reduction for its integration of enzyme production and saccharification steps in one reaction. Thus, the CBS process has the potential to lead lignocellulose bioconversion into the real world but still need further improvement.[20,25] Therefore, the development of a suitable pretreatment technology matching the cellulosome-based CBS process is of significant importance for the cost-effective production of cellulosic ethanol.

Notably, it has been known that the properties of pretreated biomass are highly related to saccharification efficiency, and the relationship between pretreatment and fungal enzymatic hydrolysis has been extensively studied in previous reports.[26–28] However, the research regarding to the impact of the properties of pretreated biomass on the efficiency of cellulosome-based whole-cell saccharification is seldom reported. For instance, it has only been reported that the HT-pretreated biomass had a very low digestibility for cellulosome-based saccharification due to the high content of lignin.[29] Furthermore, the impact of the properties of pretreated substrates on the two distinct saccharification of fungal cellulase and bacterial cellulosome systems should be different, but the comparative evaluation is scarcely reported in literatures.

Therefore, in this study, we combined AS pretreatment (for lignin removal) and HT/xylanase treatment (for hemicellulose removal) to treat wheat straw to get the substrates with different physicochemical properties, and then the effect of the sequence of the pretreatment combinations (*i.e.* the properties of pretreated substrates) on wheat straw sugar release for both fungal cellulase and whole cell-based CBS was comprehensively evaluated and compared. In addition, detailed characterizations of both liquid and solid fractions after pretreatment were employed, in order to find why the two saccharification systems had different ability to release sugars based on the same pretreated substrates. This work is of great importance for the development of suitable pretreatment technologies to match cellulosome-based whole-cell saccharification for the cost-effective production of sugar platform, which can be further converted to fuels (*e.g.*, ethanol) or chemicals (*e.g.*, diols) with the concept of integrated biorefinery.[30,31]

2. Experimental section

2.1 Materials

Wheat straw was collected from Anhui province, China. The moist straw with water content of 66.5% was milled by a pilot twin-screw extrusion device (self-designed; manufactured by Tianzheng Screening Pulping Equipment Co., Ltd., Hebei China; the maximum throughput was 200 kg h^{-1}) without addition of any chemicals before the following experiments. The main chemical composition of wheat straw was determined according to the National Renewable Energy Laboratory (NREL) analytical procedure, and the results are shown in Table 1. All analytical-grade chemical reagents were used as received. The cellulase and xylanase used for enzymatic hydrolysis were provided by Qingdao Vland Biotech Inc. (China), and their corresponding activities were 86 FPU per mL (80 mg protein per mL) and 13 200 U per g (16 mg protein per g), respectively. The enzyme activity was measured on the basis of the standard method.[32] The *C. thermocellum* strains ΔpyrF::KBm were cultivated in GS-2 medium with 5 g L^{-1} Avicel as the sole carbon source at 55 °C for 48 h before saccharification.

2.2 Pretreatment

In this work, to remove both lignin and hemicellulose of wheat straw for the improvement of substrate accessibility, three

Table 1 Wheat straw composition and the biomass recovery after pretreatment

Samples	Composition (%)							Biomass solid recovery % (±0.5)
	Glucan (±1.0)	Xylan (±0.5)	Araban (±0.1)	AIL[a] (±0.5)	ASL[b] (±0)	Extractives[c] (±0.5)	Ash (±0.2)	
Raw	31.3	12.8	2.3	19.5	0.7	21.5	11.2	—
AS	47.0 (85.1%)	19.3 (85.3%)	1.4 (35.8%)	9.3 (27.1%)	0.9 (73.5%)	9.8 (26.0%)	7.6 (38.9%)	56.7
AS + HT	54.3 (73.8%)	13.1 (43.3%)	0 (0%)	7.0 (15.4%)	0.6 (38.3%)	10.1 (20.1%)	5.7 (21.6%)	42.5
AS + X	58.1 (83.1%)	13.0 (45.4%)	0.7 (14.5%)	8.4 (19.4%)	1.2 (72.6%)	9.8 (20.4%)	6.7 (27%)	44.8
HT	40.6 (84.9%)	10.9 (55.4%)	0 (0%)	21.1 (70.9%)	0.8 (77.4%)	13.8 (42%)	7.1 (41.7%)	65.4
HT + AS	53.0 (78.3%)	11.9 (42.7%)	0 (0%)	12.2 (29.0%)	0.8 (49.5%)	13.7 (29.4%)	6.8 (28.3%)	46.3

[a] Acid soluble lignin. [b] Acid insoluble lignin. [c] Hot water soluble and hot ethanol soluble material. The data in bracket is the recovery rate of the corresponding component based on raw material after pretreatment.

combined pretreatment approaches were designed, *i.e.*, ammonium sulfite + hydrothermal pretreatment (AS + HT), AS + xylanase hydrolysis pretreatment (AS + X), and hydrothermal + AS pretreatment (HT + AS). For each combination, the process conditions of AS, HT, and X treatments were identical, and the selected conditions were based on our previous work.[22,33] The pretreated samples were named as AS, HT, AS + HT, AS + X, and HT + AS, accordingly.

In brief, the AS pretreatment was conducted at 160 °C for 60 min with 20% (w/w, based on dry substrates) dosage of AS and 6 : 1 of liquid to solid ratio (L/S) (solid loading of 14.3 wt%). The initial concentration of AS was 3.2 wt%. The AS pretreatment was carried out in a cooking digester (VRD-42SD-A China Pulp and Paper Research Institute, Beijing, China) with four small pots with a volume of 1.5 L of each pot. Upon completion of reaction, the pots were cooled down with tap water immediately. The spent liquor was squeezed out using screen cloth (with 300 mesh) and the pretreated wheat straw samples were washed with tap water until pH reached neutral. Finally, both the washed solid residue and the spent liquor of AS pretreatment were collected and stored at 4 °C for further treatment and analysis.

The hydrothermal (HT) pretreatment was implemented at 175 °C for 20 min with 3% (w/w, based on dry substrate) dosage of acetic acid, and the L/S was 10 : 1 (solid loading of 9.1 wt%). The pretreatment reactor, the solid and liquid separation, the washing of solid, as well as the sample collection were handled following the method mentioned above.

The xylanase (X) hydrolysis was performed at 50 °C for 24 h with 5 wt% solid loading and enzyme loading of 66 U per g dry substrate (*i.e.* 0.08 mg protein per g substrate) according to our previous report.[17] The hydrolysis reaction was taken out in an incubator. After X treatments, the sample handling was carried out using the same method as mentioned above.

2.3 Fungal cellulase-based saccharification

Enzymatic hydrolysis of pretreated wheat straw was conducted with solid loading of 3 wt% at 50 °C for 72 h in serum bottles (25 mL) placed in an air bath incubator shaker at 90 rpm. The initial pH was adjusted to 4.8 with sodium citrate buffer and 0.02% (w/v) sodium azide was added to prevent microbial contamination. During enzymatic hydrolysis, the hydrolysate was sampled at desired intervals for glucose and xylose analysis. All the experiments were carried out at least three times.

2.4 Cellulosome-based consolidated bio-saccharification

A previously constructed *C. thermocellum* strain ΔpyrF::KBm[22] was grown anaerobically at 55 °C in GS-2 medium with 5 g L^{-1} Avicel (PH-101, Sigma) as the carbon source to exponential phase. The culture was concentrated to remove the cell pellets. The supernatant containing extracellular proteins was used to determine the cellulase activity by adding 15 g L^{-1} Avicel as the substrate. The released reducing sugars were monitored by the 3,5-dinitrosalicylic acid (DNS) method after incubating at 55 °C for 48 h. One unit of cellulase activity was defined as the amount of extracellular proteins required to produce 1 mg of reducing sugars per hour under certain conditions. To initiate the saccharification process, 1 mL culture was inoculated into 100 mL medium containing 3 g dry pretreated wheat straw. 1 mL sample was taken from each setup every 2 days to determine the released glucose and xylose by high performance liquid chromatography (HPLC).[34] Three independent experiments were prepared for every condition.

2.5 Composition analysis

The composition of native and treated wheat straw was measured using two-step sulfuric acid hydrolysis according to the NREL procedures.[35] Acidic and enzymatic hydrolyzates (0.22 μm filtered) were analyzed by HPLC system (Model 1200, Agilent, USA) equipped with a Bio-Rad Aminex HPX-87H column (300 mm × 7.8 mm) and refractive index detector. The column was operated at 55 °C with 0.005 M/L H_2SO_4 solution as the mobile phase at a flow rate of 0.6 mL min^{-1}. The losses of sugar degradation in acid hydrolysis were corrected by subjecting known amounts of standard sugars through the same test procedures. The calibration curve was built by subjecting the known and gradient concentrations of standard sugars, and at least five different concentration points were set and measured. The content of furfural (FF) and 5-hydroxymethyl furfural (HMF) in hydrolyzates was measured by HPLC (Waters 2489, USA) with ultraviolet detector (284 nm) and SunFire C18 (4.6 mm × 250 mm) chromatographic column. Ethanol/water

(volume ratio of 1 : 4) was used as mobile phase with a flow rate of 1 mL min^{-1} at 35 °C. All samples were analyzed at least in duplicate and the average was reported.

The biomass solid recovery ($R_{biomass}$) after pretreatment was calculated as the following eqn (1), the recovery rates of glucan (R_{glucan}), xylan (R_{xylan}) and total sugar (glucan + xylan) ($R_{total\ sugar}$) after pretreatment were calculated as the eqn (2)–(4), the delignification rate (D_{lignin}) of pretreatment was computed using the eqn (5), the enzymatic digestibility of glucan (E_{glucan}), xylan (E_{xylan}), and total sugar (glucan plus xylan) ($E_{total\ sugar}$) in substrates for enzymatic hydrolysis were calculated as the eqn (6)–(8), and the total sugar digestibility for *C. thermocellum* saccharification ($C_{total\ sugar}$) was computed following the eqn (9).

$$R_{biomass}(\%) = \frac{W_{residual\ wheat\ staw\ after\ pretreatment}}{W_{orignal\ wheat\ straw}} \quad (1)$$

$$R_{glucan}(\%) = \frac{W_{glucan\ in\ pretreated\ wheat\ staw}}{W_{glucan\ in\ orignal\ wheat\ straw}} \quad (2)$$

$$R_{xylan}(\%) = \frac{W_{xylan\ in\ pretreated\ wheat\ staw}}{W_{xylan\ in\ orignal\ wheat\ straw}} \quad (3)$$

$$R_{total\ sugar}(\%) = \frac{W_{glucan\ plus\ xylan\ in\ pretreated\ wheat\ staw}}{W_{glucan\ plus\ xylan\ in\ orignal\ wheat\ straw}} \quad (4)$$

$$D_{lignin}(\%) = 1 - \frac{W_{lignin\ in\ pretreated\ wheat\ staw}}{W_{lignin\ in\ orignal\ wheat\ straw}} \quad (5)$$

$$E_{glucan}(\%) = \frac{W_{glucose\ in\ enzymatic\ hydrolysate} \times 0.9}{W_{glucan\ in\ pretreated\ wheat\ straw}} \quad (6)$$

$$E_{xylan}(\%) = \frac{W_{xylose\ in\ enzymatic\ hydrolysate} \times 0.88}{W_{xylan\ in\ pretreated\ wheat\ straw}} \quad (7)$$

$$E_{total\ sugar}(\%) = \frac{W_{glucose\ in\ enzymatic\ hydrolysate} \times 0.9 + W_{xylose\ in\ enzymatic\ hydrolysate} \times 0.88}{W_{glucan\ and\ xylan\ in\ pretreated\ wheat\ straw}} \quad (8)$$

$$C_{total\ sugar}(\%) = \frac{W_{glucose\ in\ cellulosome\ hydrolysate} \times 0.9 + W_{xylose\ in\ cellulosome\ hydrolysate} \times 0.88}{W_{glucan\ and\ xylan\ in\ pretreated\ wheat\ straw}} \quad (9)$$

where, W is the mass of corresponding components (g). The coefficients of 0.9 and 0.88 were the conversion factors for the conversion of glucan and xylan into glucose and xylose, respectively. All the experiments were performed at least in triplicates, and average data were reported.

2.6 Molecular weight and distribution of lignin

The molecular weight and distribution of lignin in spent liquor after AS pretreatment were characterized by gel permeation chromatography (GPC, HELEOS System, Wyatt Co., USA) with differential detector and laser detector. 0.1 mol L^{-1} $NaNO_3$ was used as mobile phase with a flow rate of 1.0 mL min^{-1}. Standard sodium polystyrene sulfonate was utilized for calibration.

2.7 Organic element analysis of lignin

The elements of C, H, O, N and S in lignin obtained from AS pretreatment were analyzed on an elemental analyzer (Vario EL cube, Elementar Co., Germany) through burning with oxygen at temperature of 1200 °C for 70 s.

2.8 Fourier transform infrared spectroscopy (FTIR) analysis

FTIR spectra of intact and pretreated wheat straw as well as lignin samples were obtained on a Nicolet 6700 FTIR Spectrometer (Thermo, USA). The sample was prepared through KBr pellet, and the weight ratio of KBr to sample was 100 : 1. Spectra were collected at a resolution of 4 cm^{-1} in the range of 500 to 4000 cm^{-1}, and 32 scans per sample were conducted. The absorption peaks at 2900, 1430, 1372, and 897 cm^{-1} of wheat straw were used for the calculations of cellulose crystalline index according to the following equations.[36,37]

$$TCI = A_{1372}/A_{2900} \quad (10)$$

$$LOI = A_{1430}/A_{897} \quad (11)$$

where, TCI is the total crystallinity index, LOI is the lateral order index, and A is absorbance value of the corresponding absorbance peak.

2.9 ^{1}H–^{13}C 2D-HSQC nuclear magnetic resonance (NMR) spectroscopy analysis

The AS spent liquor mainly composed of lignin was desalted and then 2D-HSQC NMR spectra were determined by an AVANCE-III 600 MHz spectrometer (Bruker, Switzerland). 20 mg lignin sample was dissolved in 0.6 mL of D_2O. The spectral widths were 5000 and 20 000 Hz for the ^{1}H and ^{13}C dimensions, respectively. Integration calculations of the 2D contours in all spectra were performed using MestReNova software.

2.10 X-ray diffractometer measurement

Crystallinity of intact and treated wheat straw was determined by a D8 ADVANCE X-ray diffractometer (XRD, Bruker Co., Germany) equipped with Ni-filtered Cu Kα radiation generated at 40 kV and 40 mA. The scattering angle range was 5–60° with a scanning rate of 4° min^{-1}. The crystallinity index (CrI) was calculated according to the empirical method developed by Segal and coworkers.[38]

2.11 Porosity of substrates analysis

The dye adsorption method was used to semi-quantitatively measure the porosity of pretreated substrates.[27] In brief, 0.1 g (oven dry) pretreated wheat straw was put into glass tubes (20 mL) and the required amount of distilled water was added with a L/S of 100 : 1 at various dye concentrations (0.5–5%, based on the dry weight of wheat straw), which can be used to measure

the dye adsorption isotherm. The dye applied in this study was Congo red with a molecular size of 2.6 nm. The wheat straw was dyed in an incubator shaker at 60 °C with a speed of 90 rpm for 24 h. After dyeing, the samples were centrifuged at 9000 rpm for 5 min to remove cellulosic substrates. The absorbance of supernatant was tested with a UV-Visible spectrophotometer (UV-3000, China) at the wavelength of 492 nm for Congo red.[39] The amount of dye absorbed by wheat straw was determined from the decrease in concentrations of the dye solution after dyeing and was computed as mg dye per g pretreated wheat straw.

2.12 Scanning electron microscopy analysis

The surface morphology and element distribution of treated wheat straws were observed by scanning electron microscopy mapping (SEM-mapping, Hitachi S-4800, Japan) and Energy Dispersive Spectrometer (EDS) at 3.0 kV. Dried samples were sputter-coated with a thin gold layer prior to analysis.

2.13 Surface chemical composition and component distribution

X-ray photoelectron spectra (XPS) of pretreated wheat straws were obtained with an ESCALAB 250Xi instrument (Thermo, USA) equipped with a monochromatic Al Kα X-ray source (1486.6 eV) operated at 150 W. The full scanning range was from −10 to 1350 eV with the pass energy of 50 eV. C 1s peak (E_b = 284.8 eV) was used as E_b charge calibration of samples. At least three different spots were measured on each sample. The oxygen-to-carbon (O/C) ratios were calculated from the low resolution XPS spectra. The surface coverage by lignin (S_{lig}) and carbohydrates (S_{car}) were calculated according to the following equations respectively, using the average O/C ratio value.[40]

$$S_{lig}\% = (O/C_{sample} - O/C_{carbohydrate})/(O/C_{lignin} - O/C_{carbohydrate}) \times 100 \quad (12)$$

$$S_{car}\% = 1 - S_{lig}\% \quad (13)$$

Among of which, $O/C_{carbohydrate} = 0.83$, $O/C_{lignin} = 0.33$.

3. Results and discussion

3.1 Compositional analysis of raw and pretreated wheat straw

The chemical composition of raw and pretreated wheat straw and the biomass recovery after pretreatment are shown in Table 1. To be visualized, the major contents of glucan, xylan, lignin, and other compounds (including ash and extractives) as well as the solid recovery of each pretreated wheat straw are normalized on a basis of 100 g raw feedstock (Fig. 1). Because of the very low amount of araban compared to glucan and xylan, the change of araban is not shown in Fig. 1. It can be observed that AS pretreatment was effective in delignification, which was due to the cleavage of C–C bond between lignin macromolecules and lignin–carbohydrate compound (LCC) by sulfonation or ammonolysis.[12] Moreover, the sulfonated lignin became more

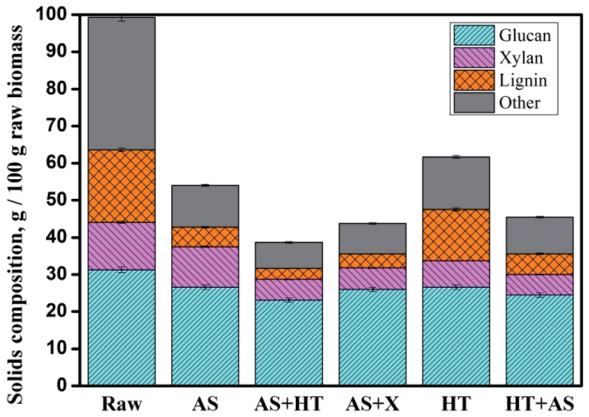

Fig. 1 The mass of glucan, xylan, lignin and other compounds in the raw and pretreated wheat straw based on 100 g feedstock.

hydrophilic and was liable to be dissolved out. Table 1 exhibits that approximately all araban and half of xylan was removed through HT pretreatment because of the acetic acid hydrolysis. After two-step pretreatment process, the sequence of biomass solid recovery was AS + HT (42.5 ± 0.3%) < AS + X (44.8 ± 0.2%) < HT + AS (46.3 ± 0.3%). The lignin content (7.04%) of AS + HT pretreated wheat straw was comparable to the one (8.42%) with AS + X pretreatment, while both of which were obviously lower than that (12.24%) of HT + AS pretreated wheat straw. Correspondingly, the delignification rates with AS + HT (84.6%) and AS + X (80.6%) pretreatments were all higher than that with HT + AS (71%) pretreatment, as shown in Fig. 1.

In addition, although the determination of extractives after HT pretreatment was not accurate because the condensed lignin could be easier to be extracted by ethanol, the removal of extractives and ash was beneficial to the increase of enzyme accessibility in the subsequent saccharification.[33] With regard to the recovery rates of glucan, xylan, and total sugars, the AS + X pretreatment method was the highest among the three approaches (Fig. 2), because the condition of xylanase treatment (50 °C) was rather milder compared to HT pretreatment (175

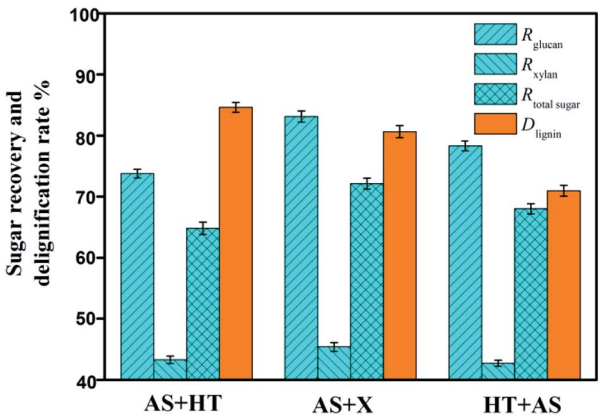

Fig. 2 Effect of two-step pretreatments on the recovery rates of glucan (R_{glucan}), xylan (R_{xylan}) and total sugar ($R_{total\ sugar}$) and the delignification rate (D_{lignin}).

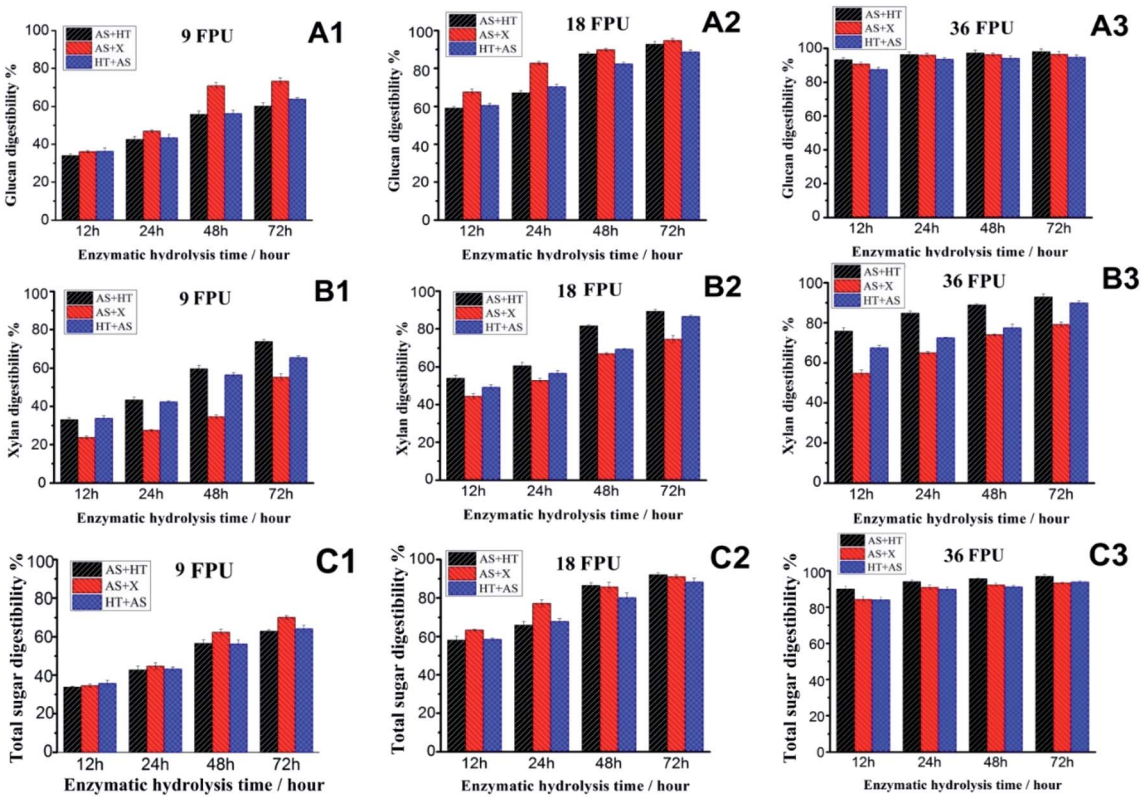

Fig. 3 Digestibility of pretreated wheat straw as the function of enzymatic hydrolysis time with different cellulase loadings (A1–A3: glucan digestibility with cellulase loading of 9, 18, and 36 FPU per g per glucan, respectively; B1–B3: xylan digestibility with cellulase loading of 9, 18, and 36 FPU per g per glucan, respectively; C1–C3: total sugar (glucan + xylan) digestibility with cellulase of loading of 9, 18, and 36 FPU per g per glucan, respectively).

°C). Milder conditions could avoid severe degradation of carbohydrates.

3.2 Comparative evaluation of the effect of pretreatment combinations on fungal cellulase-based and whole-cell-based saccharification

Two distinctive saccharification methods, the fungal cellulase-based enzymatic hydrolysis and the whole-cell biocatalyst-based CBS, were adopted respectively to evaluate the sugar release of the substrates obtained by different pretreatment combinations.

For fungal cellulase-based saccharification, the effects of cellulase dosage and digestion duration on sugar release of the three pretreated wheat straw were comparatively investigated. As can be seen from Fig. 3(A1–A3), the glucan digestibility of AS + X pretreated wheat straw overmatched the other samples with a relatively lower cellulase dosage (9 FPU per g per glucan (8.4 mg protein per g per glucan)). When the cellulase dosage was 18 FPU per g per glucan (16.7 mg protein per g per glucan), the glucan digestibility of AS + X pretreated wheat straw was still higher than the other samples in the first 24 hours hydrolysis, while after saccharification for 48 hours the glucan digestibility of AS + HT and HT + AS pretreated wheat straw samples was nearly paralleled to the AS + X pretreated wheat straw. These phenomena were due to the difference of substrate properties (particularly for the surface properties).[41] The clear difference on the digestibility of the pretreated samples (particularly with a lower cellulase dosage) was not only related to the total amounts of chemical compositions (*e.g.*, total lignin content), but also dependent on the surface properties of substrate (*e.g.*, surface lignin, pore size), which were comprehensively characterized and will be discussed in the following sections. In addition, with the cellulase dosage of 36 FPU per g per glucan (33.5 mg protein per g per glucan), the glucan digestibility of the three pretreatment approaches all reached the highest level in a relatively short hydrolysis time, which were 93.3%, 90.7%, and 87.5% for AS + HT, AS + X, and HT + AS pretreatment respectively after 12 hours digestion. The over charged cellulase loading with prolonged saccharification can reduce/cover up the difference of substrate digestibility, but the over charged enzyme will significantly increase the cost of saccharification.

Also, the xylan digestibility of AS + X pretreated substrate was obviously lower than the other two samples (Fig. 3B1–B3), implying that the remaining hemicellulose in AS + X pretreated straw had a lower accessibility to enzymes. This result was because part of accessible hemicellulose was already digested during the stage of X (xylanase) treatment. In addition, the xylan digestibility of HT + AS substrate was slightly lower than that of AS + HT substrate. This was because the HT + AS substrate with a relatively higher lignin content (Table 1) had a relatively lower enzyme accessibility.

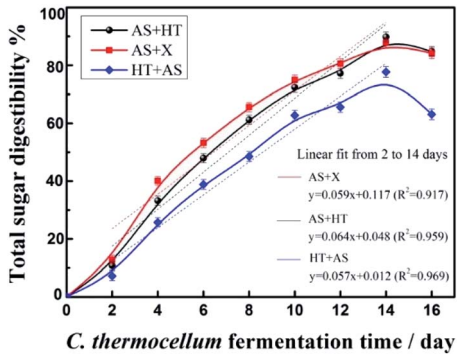

Fig. 4 Total sugar digestibility of the three pretreated wheat straw saccharified by *C. thermocellum* cellulosome.

In addition, the total sugar (glucan + xylan) digestibility (Fig. 3C1–C3) had similar changes and trends to the glucan digestibility, because glucan was the main polysaccharide in pretreated wheat straw (Table 1). The highest total sugar digestibility for AS + HT, AS + X and HT + AS pretreated wheat straw approached to 97%, 93.3%, and 93.8% respectively, after hydrolyzing for 48 h with cellulase loading of 36 FPU per g per glucan (33.5 mg protein per g per glucan), showing comparable saccharification efficiency. These results were substantially higher compared to the untreated wheat straw (19.6%) under the same saccharification conditions. Yet, the over charged cellulase loading is not economically feasible. In general, the effects of the sequence of pretreatment combinations on sugar release showed a slight influence on the saccharification using fungal cellulase.

For cellulosome-based CBS process using engineered *C. thermocellum* strain as the whole-cell biocatalyst, the whole saccharification process was initiated by inoculating 1 mL preculture with cellulase activity of 34.38 U per mL and last for 14 days (Fig. 4). According to our previous study,[23] the CBS process contains two stages, cell-cultivation stage and cellulose hydrolysis stage. In the first stage which lasts for 36 h, the inoculated *C. thermocellum* cells consume some substrate (<0.5 wt%) to growth and produce cellulosome proteins. The amount of the cellulosome would increase significantly, although the cellulase activity and protein loading could not be determined because the produced cellulosomes would closely interact with the substrate through the carbohydrate binding modules.[42] At the end of the first stage, the pH value of the saccharification system decreased to about 6 (the initial pH was 7.4), which resulted in the cease of cell growth. Nevertheless, the cellulosome maintains the cellulolytic activity for cellulose degradation in the second stage which can last for several days.[22]

Compared to fungal cellulase-based saccharification which showed less sensitivity to different pretreated substrates (Fig. 3C1–C3), significant difference was observed for cellulosome-based whole-cell saccharification. The total sugar digestibility of AS + X pretreated substrate was higher than that of the AS + HT or HT + AS pretreated substrate before 12 days. However, the total sugar digestibility of the AS + X and AS + HT pretreated samples were comparable, and were obviously higher (over 10% higher) than that of the HT + AS pretreated sample. This phenomenon might be due to the natural difference between fungal cellulase and cellulosome. As a multiprotein complex, the cellulosome with a bigger size may need a higher accessibility of the substrate compared to the smaller free cellulases.[43] Also, the higher lignin content (about 13%) in the HT + AS pretreated substrate could form a strong barrier for the cellulosome to access to cellulose. This phenomenon indicated that the lignin content in pretreated substrate should be reduced to a certain extent to meet the requirement of cellulosome-based whole-cell saccharification. In addition, the highest total sugar digestibility of the treated wheat straw with AS pretreatment alone (without any further treatment) was only 73.5%, which was clearly lower compared to the one with AS + HT/X pretreatment. This result was due to the relatively high content of xylan (19.3%) in the AS pretreated wheat straw.[22]

Besides the lignin content, the saccharification efficiency could also be affected by the structure, functional groups, distribution, and S/G value of remaining lignin.[44] Thus, the properties of both solid and liquid fractions after each pretreatment were comprehensively characterized, and the influencing mechanism of substrate property on cellulosome-based whole-cell saccharification and fungal cellulase-based hydrolysis was comprehensively compared and discussed in the following sections of this report.

3.3 Mechanism analysis of digestibility improvement for AS + HT/X pretreatment on cellulosome-based whole-cell saccharification

3.3.1 Analysis of the spent liquor of AS pretreatment. Shown in Table 2 are the properties of the spent liquor of AS pretreatment with different pretreatment combinations. As can be seen, in the first step of AS + HT/X pretreatment, the solid content (8.17%) of the spent liquor from the AS pretreatment of raw wheat straw was higher than the one (5.8%) with the AS pretreatment of HT-pretreated wheat straw (the second step of HT + AS pretreatment). This result was because more lignin were dissolved in the spent liquor of the first step of AS + HT/X pretreatment. Also, the nitrogen and sulfur ratio in the spent liquor of AS pretreatment of original wheat straw were relatively lower, which was due to the relatively higher content of the dissolved solid fraction (*i.e.* lignin, extractives, ash) in comparison with the one derived from the second step of HT-AS pretreatment.

In addition, the molecular weights (M_w and M_n) and the polydispersity index (PDI, M_w/M_n) of the spent liquor derived from AS pretreatment were determined (Table 2 and Fig. S1†). It was mainly composed of lignin degraded by sulfonation and ammonolysis. Because the spent liquor was mixture, the molecular weights (M_w) were relatively higher compared to lignin probably due to the presence of lignin–carbohydrate complex (LCC) which could be higher than 30 000 for non-wood materials.[45] Also, both the molecular weight and the PDI of the spent liquor from the second step of HT + AS pretreatment was higher compared to the one from the first step of AS + HT/X

Table 2 Properties of the spent liquor of AS pretreatment

	Spent liquor of AS pretreatment[a]	Spent liquor of post AS pretreatment[b]
Dissolved solid (wt%)	8.17 ± 0.07	5.80 ± 0.05
pH	7.62 ± 0.03	7.52 ± 0.03
N% (wt%)[c]	8.41 ± 0.06	12.18 ± 0.09
S% (wt%)[c]	9.78 ± 0.08	15.34 ± 0.11
M_w	29 660 ± 380	52 630 ± 750
M_n	11 940 ± 120	12 280 ± 110
PDI	2.48 ± 0.02	4.29 ± 0.04
Molecular weight distribution	6000–25 000 g mol^{-1} (74.0%)	1800–36 000 g mol^{-1} (88.0%)
	25 000–100000 g mol^{-1} (23.0%)	36 000–360000 g mol^{-1} (8.4%)
	>100 000 g mol^{-1} (3.0%)	>360 000 g mol^{-1} (2.6%)

[a] Spent liquor derived from the first step of AS + HT/X pretreatment. [b] Spent liquor derived from the second step of HT + AS pretreatment. [c] Data based on the dissolved solid fraction in the spent liquor.

pretreatment, while it is observed from the Table 3 that the content of inhibitors such as 5-hydroxymethyl furfural (HMF), furfural (FF), formic acid (FA) and acetic acid (AA) in the liquid of the first step of HT + AS pretreatment were all much higher than that from the second step of AS + HT pretreatment.

3.3.2 FT-IR analysis of lignin in AS pretreatment spent liquor. Delignification is the dominant reaction in AS pretreatment. Thus, the solid fraction of spent liquor was characterized by FT-IR to analyze the changes in chemical structure of lignin derived from the first step of AS + HT/X and the second step of HT + AS pretreatment combinations. The corresponding spectra are shown in Fig. 5. The typical signal from aromatic ring of lignin appeared at 1652 cm^{-1}, 1515 cm^{-1} and 1402 cm^{-1}.[46] The band at 1402 cm^{-1} was associated with C–N stretching vibration in primary amides, and it could become sharper after ammoxidation and ammonolysis of lignin.[47] It was notable that the bands at 1042 cm^{-1} of the lignin from the first step of AS + HT/X pretreatment, assigned to S=O and S–O stretching in –SO_3H group, were relatively stronger compared to the lignin from the second step of HT + AS pretreatment,[48] indicating a deeper sulfonation degree of the lignin from the first step of AS + HT/X pretreatment. From the FT-IR characterization results, it can be verified that the lignin in biomass can be removed by sulfonation and ammonolysis during AS pretreatment. Also, the hydrophilicity of the residual lignin could be increased due to the sulfonation, which could lead to the reduction of non-productive hydrophobic adsorption of enzymes.[7] Therefore, the lignin in AS + HT/X pretreated wheat straw with a relatively higher sulfonation was beneficial to the enzymatic saccharification.

3.3.3 2D HSQC NMR analysis of lignin in the spent liquor of AS pretreatment. 2D HSQC NMR technique is a powerful tool for the detailed understanding of lignin structure, allowing for the resolution of overlapping resonances observed in either the ^{1}H or ^{13}C NMR spectra. In order to acquire a more complete understanding of the lignin structures, 2D HSQC NMR spectra of lignin samples from the first step of AS + HT/X pretreatment and the second step of HT + AS pretreatment were comparatively investigated. The side-chain regions (δ_C/δ_H 50–90/2.5–6.0) and the aromatic regions (δ_C/δ_H 100–135/5.5–8.5) of the HSQC spectra of these two lignin fractions are shown in Fig. 6. The main substructures are depicted in Fig. 7, and the main lignin cross-signals assigned in the HSQC spectra comparing with the previous literatures[49,50] are listed in Table S1.†

Table 3 Composition of the liquids derived from hydrothermal or xylanase pretreatment[a]

Classification	Component	HT (ppm)	AS + HT (ppm)	AS + X (ppm)
Monosaccharide	Glucose	268	317.2	178
	Xylose	92	118.8	466.8
	Arabinose	284	501.6	0
Polysaccharide	Glucan	1336	242.8	0
	Xylan	9508	7417	5865
	Araban	456	286.4	495.2
Inhibitor	HMF	94	30.4	ND
	FF	492	320	ND
	FA	198.4	0	0
	AA	1194	1068	0

[a] HMF: 5-hydroxymethyl furfural; FF: furfural; FA: formic acid; AA: acetic acid; ND: not detected.

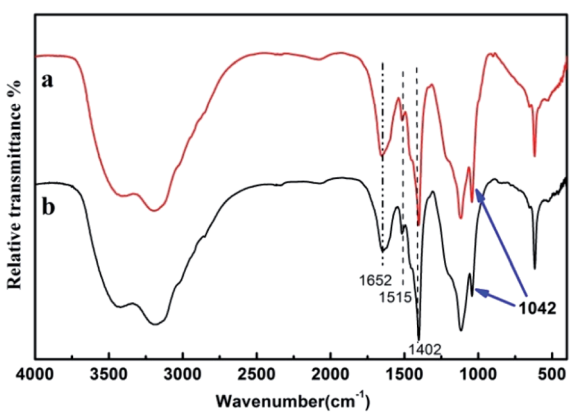

Fig. 5 FT-IR spectra of lignin in AS pretreatment spent liquor ((a): lignin from AS + HT/X pretreatment; (b): lignin from HT + AS pretreatment).

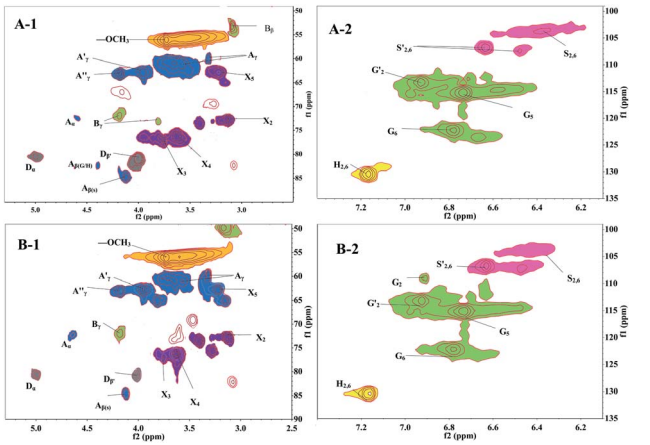

Fig. 6 Side-chain (left column, δ_C/δ_H 50–90/2.5–5.3) and aromatic regions (right column, δ_C/δ_H100–135/6.0–7.4) of lignin in the 2D HSQC NMR spectrum (A-1, A-2: lignin from the first step of AS + HT/X pretreatment; B-1, B-2: lignin from the second step of HT + AS pretreatment. Signal assignments are listed in Table S1†).

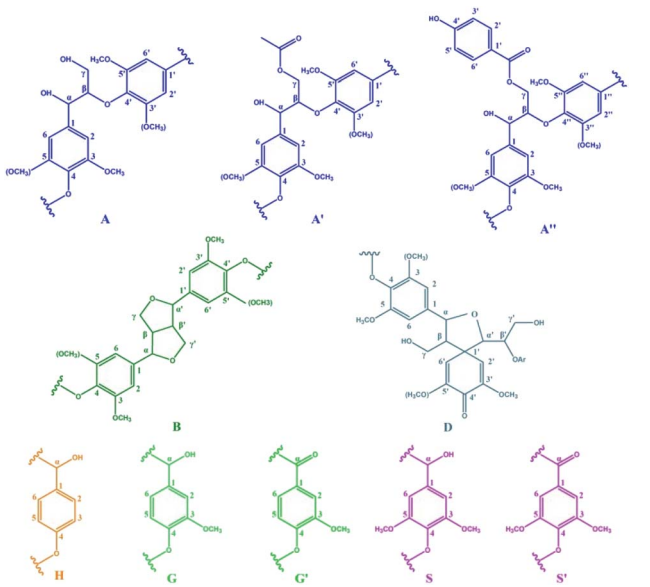

Fig. 7 Main classical substructures involving different side-chain linkages and aromatic units identified by 2D NMR of lignin in spent liquor of AS pretreatment.

The side-chain region (δ_C/δ_H 50–90/2.5–6.0) of the spectra provided useful information about the interunit linkages presented in lignin. The main signals were from methoxyls, β–O-4′, β–β′, β-5′, β-1′, and 5–5′ linkages. As shown in Fig. 6 (left column), the side-chain regions of these two lignin fractions in the HSQC spectra were similar. Both spectra showed prominent signals corresponding to methoxyls (δ_C/δ_H 56/3.73) and β–O-4′ aryl ether linkages.

The C–H correlation in β–O-4′ substructures (A) were assigned for α-, β-, and γ-C positions at δ_C/δ_H 71.8/4.6 (C_α–H_α), 82.9/4.38 (C_β–H_β linked to G and H units), 84.6/4.13 (C_β–H_β linked to S unit) and 59.86–60.97/3.31–3.65 ppm (C_γ–H_γ), respectively. The γ-acylated β–O-4′ substructures (A′ and A″) were detected at the signals of δ_C/δ_H 62.8/3.96 (C_γ–H_γ) and 63.11/4.18 (C_γ–H_γ) ppm. In addition, strong signals for resinol (β–β′) substructures B were observed with their C_β–H_β and the double C_γ–H_γ correlations at δ_C/δ_H 53.28/3.09 and 71.0/3.8 and/4.2, respectively. The signals corresponding to spirodienone (β-1′) substructures D could be observed at 80.8/5.07 (C_α–H_α) and 80.8/4.01 ppm (C_β–H_β). Whereas the phenylcoumaran (β-5′) substructures were not discovered in both of the side-chain region spectra.

Signals assigned to *p*-hydroxyphenyl (H), guaiacyl (G) and syringyl (S) lignin units were mainly in the region of δ_C/δ_H 100–135/5.5–8.5. The ^{13}C–^{1}H correlations for $S_{2,6}$ and $S'_{2,6}$ were at δ_C/δ_H 103.9/6.37 and δ_C/δ_H 106.9/6.64, respectively. The G unit showed diverse correlations for C_2–H_2, C_5–H_5 and C_6–H_6 at δ_C/δ_H 107.5/6.48, 115.3/6.74 and 122.3/6.79 ppm, respectively. The oxidized (C_α=O) structure G′ (for the C_2–H_2) was assigned to the signal at δ_C/δ_H 113.2/6.92 ppm, and the resonance from $H_{2,6}$ was observed at δ_C/δ_H 130.5/7.17.

Moreover, various signals from the associated carbohydrates could also be found in the HSQC spectra. In the aliphatic regions (Fig. 6, left column), signals from β-D-xylopyranoside units (X) were evidently noted, with its C_2–H_2 (X_2), C_3–H_3 (X_3), and C_4–H_4 (X_4) correlations at δ_C/δ_H 72.8/3.13, 77.46/3.76, and 76.35/3.63, respectively.

The different structural features of these two lignin fractions were quantitatively investigated. The percentages of lignin side chains involved in the primary substructures and the S/G ratios were calculated from the corresponding HSQC spectra, and the results are listed in Table 4. As expected, the main substructures present in both of these two lignin fractions were the β–O-4′ linked ones (A, A′, and A″), with 79.8% and 88.1% for the lignin from the first step of AS + HT/X pretreatment and the second step of HT + AS pretreatment, respectively. It was apparent that the amount of β–β′ resinol substructure (B) and β-1′ spirodienone substructure (D) of the lignin from the first step of AS + HT/X pretreatment were higher than that of the lignin from the second step of HT + AS pretreatment, suggesting that more types of lignin could be dissolved out in the first step of AS + HT/X pretreatment. These results are in line with the chemical component analysis shown in Table 1.

In addition, the S/G ratio is an important parameter to monitor the behaviors of lignin de-polymerization and elucidate the degradation mechanism.[51] As known, the larger of the S/G value, the less of the condensed lignin could be obtained.[52] As can be observed in Table 4, the S/G value (0.56) of the lignin sample from the first step of AS + HT/X pretreatment was higher than that of the lignin (0.49) from the second step of HT + AS pretreatment, which was attributed to the fact that the lignin from the first step of AS + HT/X pretreatment was mainly composed of the degraded lignin fragments. It was implied that the ether linked S unit was more susceptible to be cleaved in the first step of AS + HT/X pretreatment, thus leading to a higher lignin removal.

3.3.4 Accessibility of pretreated wheat straw and the micromorphology of *C. thermocellum* with cellulosome. The XRD and FT-IR spectra of raw and pretreated wheat straw are

Table 4 Percentage of the main inter-unit linkages (referred to as the total side chains) and S/G (syringyl to guaiacyl) ratio of the lignin in the spent liquor of AS pretreatment

Lignin sample	β–O-4′	β–β′	β-1′	S/G
Lignin from the first step of AS + HT/X pretreatment	79.8%	9.9%	10.3%	0.56
Lignin from the second step of HT + AS pretreatment	88.1%	3.6%	8.3%	0.49

depicted in Fig. S2 and S3,† respectively. And the corresponding attribution of peak signals in FT-IR spectra of the raw and pretreated wheat straw samples are shown in Table S2.†

CrI of entire material (including cellulose, hemicellulose, lignin, and other components) was considered as a crucial factor that can influence the enzymatic saccharification of lignocellulosic biomass.[53] The CrI of raw wheat straw was 43.6%, which was lower compared to the pretreated wheat straw (47.2–55.8%) (Table 5). The increase of CrI after pretreatment was mainly because of the removal of amorphous components (*e.g.* lignin, hemicelluloses, extractives),[54] which was consistent with chemical composition results (Table 1). It was depicted that the CrI of AS + X (55.8%) and AS + HT (53.5%) pretreated straw were both higher than that of HT + AS (52.3%) pretreated straw, indicating a higher content of crystalline cellulose in the former two samples, which could have positive effect on *C. thermocellum* cellulosome saccharification, but have little impact on cellulase saccharification. Our previous studies have shown that higher content of crystalline cellulose in substrate was preferred for the cellulosome-based whole cell saccharification in comparison with fungal cellulase hydrolysis.[22]

It was reported that reducing cellulose crystallinity was beneficial to improve the enzymatic hydrolysis efficiency.[55] But the XRD method is difficult to measure the crystallinity of cellulose itself due to the presence of amorphous components such as hemicellulose and lignin.[56] Therefore, FTIR analysis was used to characterize the changes of cellulose crystallinity. The peaks at 1430 and 897 cm^{-1} were correlated to the crystalline structure of cellulose. The ratio of peak at 1430 to 897 cm^{-1} was referred as the lateral order index (LOI), while the ratio of peak at 1372 to 2900 cm^{-1} was known as the total crystallinity index (TCI). The corresponding LOI and TCI data are presented in Table 5. As can be observed, both the LOI and TCI for HT + AS pretreated straw samples were lower than that of AS + HT or AS + X pretreated samples, indicating that HT + AS pretreatment caused more damage to the crystalline region of cellulose probably due to the hasher pretreatment conditions. This was in agreement with the results shown in Table 3 (HT first could cause more degradation of carbohydrates). However, the pretreated wheat straw with lower crystallinity had not shown excellent performance in both cellulase and cellulosome saccharification efficiency, which was different from other studies.[57] This result indicated that slightly higher cellulose crystallinity was not the main factor compared to the lignin content or pore size of the substrate, although it would be a barrier to enzymatic hydrolysis.[5]

The dye adsorption method was used to semi-quantify the porosity of substrate, and to evaluate the accessibility of the substrate to enzyme and cellulosome.[32] As shown in Table 5, the dye adsorption value of AS + HT and AS + X pretreated samples were obviously higher than that of HT + AS pretreated sample, indicating that AS + HT/X pretreatment could generate a high porosity in the pretreated substrate. It is evident that a high porosity is beneficial to saccharification for both the free fungal cellulase with smaller size and the *C. thermocellum* cellulosome, but the Congo red with the size of 2.6 nm cannot quantitatively reflect the larger pores. As can be seen from the Fig. 8, the *C. thermocellum* had a larger size with the length of 2 μm and diameter of 0.2 μm approximately, of which the size was approximately 150 times of free enzymes,[58] and most of the cellulosome was attached to its external surface and cannot dissociate. It is known that larger pores or big open gaps of the substrate was able to enhance the access of cellulosome into substrate, and the saccharification efficiency could be improved consequently.[43] Also, it has been reported that pretreatment under severer intensities could generate a large number of ink

Table 5 Crystallinity and porosity of raw and pretreated wheat straw

Sample	CrI (%)	LOI	TCI	Dye adsorption value (mg g^{-1})
Wheat straw	43.6	0.788	1.05	205.6
AS	51.9	0.859	0.942	384.5
AS + HT	53.5	0.895	0.974	413.3
AS + X	55.8	0.853	0.987	411.8
HT	47.2	0.751	0.977	359.3
HT + AS	52.3	0.822	0.905	400.2

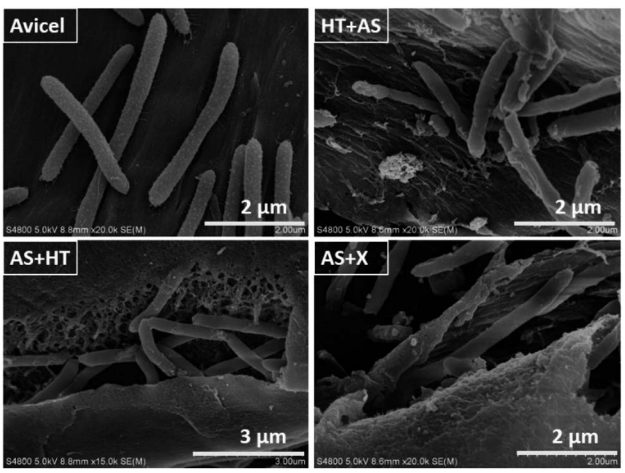

Fig. 8 SEM images of *C. thermocellum* with cellulosome on the Avicel and pretreated wheat straw saccharified after 5 days.

bottle pores or closed pores. These kinds of pores could be opened during saccharification to promote sugar release.[57] However, HT pretreatment (even post HT pretreatment after AS pretreatment) can generate re-located and condensed lignin with larger size on the surface of fiber, leading to a less probability to open the ink bottle pores or closed pores during saccharification. This is the reason why the total sugar digestibility of AS + HT pretreated substrate was relatively lower compared to the AS + X pretreated substrate for cellulosome-based whole-cell saccharification in 2–12 days (Fig. 4). In other words, the ink bottle pores or closed pores of AS + X pretreated substrate might be easier to be opened during saccharification to generate larger pores to facilitate sugar release, compared to the AS + HT pretreated substrate. Therefore, it could be concluded that cellulosome is more sensitive to substrate accessibility (particularly for large size pores) compared to cellulase.

3.3.5 Micromorphology and features of the pretreated wheat straw. The SEM images of the raw and pretreated wheat straw samples are displayed in Fig. 9. A compact plate-structure could be observed in raw wheat straw (Fig. 9 Raw), while there were many small particles or pellets (probably were condensed lignin or pseudo-lignin) on the surface of HT + AS pretreated straw, which could result in a weaker accessibility of the substrate to free cellulase especially to cellulosome.[42,59] In contrast, there were few aggregated pellets on the surface of AS + HT/X pretreated wheat straw. Additionally, looser fibers with big open gaps were observed on the AS + HT/X pretreated substrates compared with HT + AS, which was in favor of the enhancement of the saccharification, particularly for cellulosome with bigger size.[43]

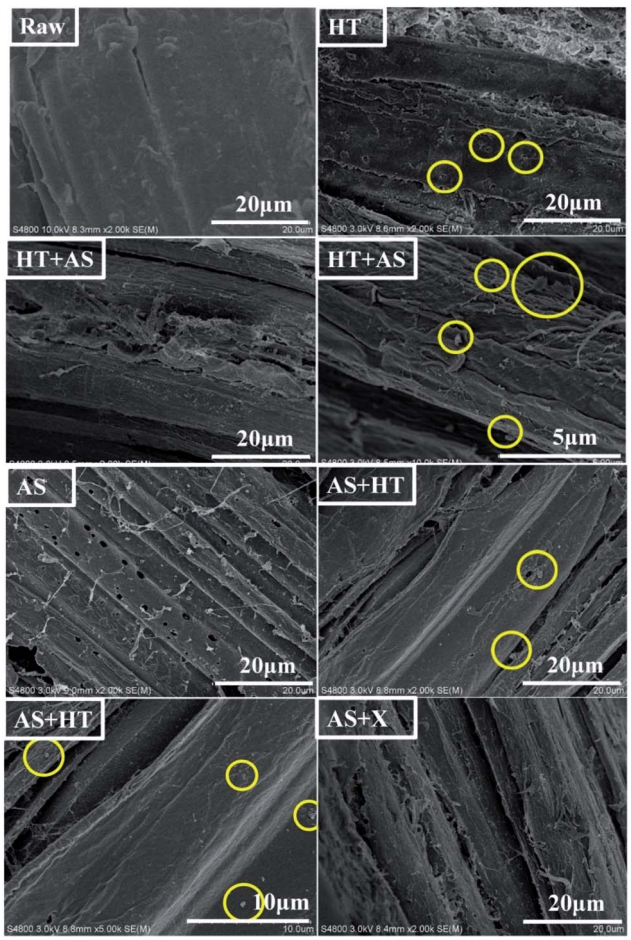

Fig. 9 SEM images of raw and pretreated wheat straw.

In order to compare the features of pretreated wheat straw, the elements content and distribution in the substrates were characterized by EDS and SEM-mapping. As shown in Table 6, the silicon ratio of the AS + HT/X pretreated wheat straw was much lower than that of the HT + AS pretreated samples, indicating an effective ash removal in AS + HT/X pretreatment. It was reported that the ash would also impede the effect of enzymatic saccharification.[60] In addition, the O/C value of the AS + HT/X pretreated wheat straw was higher than that of the HT + AS pretreated sample, due to the lower content of residual lignin, which was in agreement with the chemical composition analysis (Table 1). As displayed in Fig. 10, the elements of oxygen and silicon were uniformly distributed in the pretreated wheat straw. Obviously, the silicon accumulation in the HT + AS pretreated substrates was far more than that of the AS + HT/X pretreated substrates, which was coincident with the data of Table 6.

XPS is a surface chemical analysis instrument which is able to measure elemental compositions, chemical state and electronic state of the elements that exist in a material with a depth of about 3–10 nm.[61] It has been applied for investigating the surface coverage by lignin, carbohydrates or extractives by empirical formula.[40] The surface chemical composition of pretreated wheat straw samples with different approaches was analyzed by XPS as shown in Table 7. The elements detected were O and C and minor amounts of N and Si from natural biomass. As can be observed, the amount of silicon on the surface of AS + HT/X pretreated substrate was much lower than that of HT + AS pretreated sample, facilitating the enzymatic hydrolysis. The O/C values were used for the estimation of surface coverage by lignin or carbohydrates before and after pretreatment. As shown in Table 7, the surface lignin on the substrate pretreated by AS + HT method decreased remarkably, while it was slightly changed by HT + AS pretreatment. High surface lignin content could be a barrier for saccharification by reducing the external surface of substrate.[41]

The cellulosome is a protein complex containing multiple enzymes. Compared to the free fungal enzymes, the cellulosome is with a larger size and its accessibility might be more sensitive to the high lignin content, condensed lignin macromolecule,

Table 6 Element content (wt%) of the pretreated wheat straw characterized by EDS

Sample	C	O	Si	S	O/C
HT	56.0	38.1	5.81	0.12	0.68
HT + AS	54.82	42.61	2.17	0.16	0.77
AS	55.57	42.88	1.0	0.55	0.77
AS + HT	54.65	44.17	0.79	0.27	0.81
AS + X	55.26	43.72	0.84	0.19	0.79

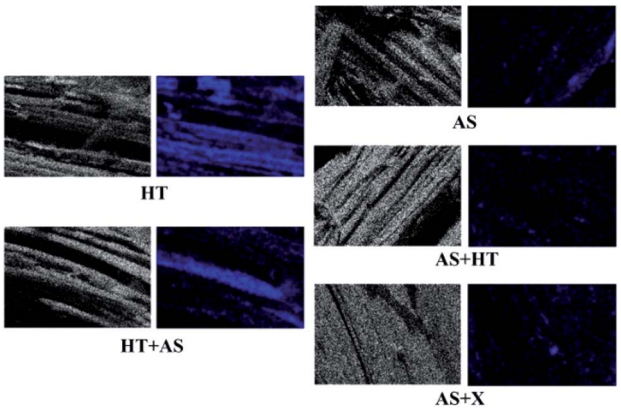

Fig. 10 Element distribution of the pretreated wheat straw characterized by SEM-mapping (white spots: (left for each sub-figure): oxygen; blue spots (right for each sub-figure): silicon).

Table 7 Surface element proportion and surface coverage by lignin (S_{lig}), carbohydrates (S_{carb}) of pretreated wheat straw characterized by XPS

Sample	Si %	C %	N %	O %	O/C	S_{lig} %	S_{carb} %
HT	2.51	63.4	1.02	33.42	0.53	62	40
HT + AS	2.16	64	0.7	33.32	0.52	60	38
AS	1.81	63.93	0.92	33.17	0.52	62	38
AS + HT	1.71	56.49	0.42	40.59	0.72	22	78
AS + X	1.81	61.03	1.1	36.06	0.59	48	52

enrichment of extractives and ash, as well as porosity and pore size of the substrate. Thus, the cellulosome-based whole-cell saccharification is more susceptible to the sequence of AS and HT pretreatment (*i.e.* the properties of substrates) in comparison with the free cellulase-based enzymatic hydrolysis. This also explained the lower efficiency of cellulosome-based saccharification compared to enzymatic hydrolysis (Fig. 3 and 4). The cellulosome-based whole-cell saccharification (also called CBS) is a newly proposed strategy which has the potential to lead lignocellulose bioconversion into the real world but still need further improvement.[20,25] Several solutions can be taken:

(1) To develop more compatible pretreatment technology based on the AS + HT method in this study to significantly increase the accessibility of pretreated substrate to cellulosome.

(2) To develop robust whole-cell biocatalysts with higher activity and adaptability by adaptation, mutagenesis, or genetic engineering of the bacteria to reduce the stringent requirements for the pretreated substrates.

(3) To promote the saccharification by supplementing small amounts of non-cellulosomal enzymes in the system. For instance, the addition of β-glucosidase may reduce the inhibition effect of cellobiose, and the addition of xylanase can greatly shorten the saccharification process.[22] Further cellulosome engineering should be carried out to improve its adaptability to the substrates with different features.

(4) To develop novel instruments and equipment to reduce mass transfer limitation particularly for high-solid loading saccharification.

4. Conclusions

In this study, two distinct biological saccharification strategies using fungal enzymes and *C. thermocellum* cellulosome were compared to evaluate the effect of the properties of substrates obtained from different pretreatment combinations based on ammonium sulfite (AS) pretreatment, hydrothermal (HT) pretreatment, and xylanase (X) pretreatment on wheat straw sugar release, and to reveal the reason why the two saccharification systems have different ability to release sugars with the same pretreated substrates. Results showed that AS + HT/X pretreatment could remove more lignin, generating large external surface and less surface lignin coverage on the substrate, thus leading to a higher accessibility to cellulosome, in comparison with HT + AS pretreatment. Therefore, AS + HT/X pretreatment is more compatible with cellulosome-based whole-cell saccharification. In addition, HT pretreatment should be carefully adjusted to reduce re-arrangement and condensation of lignin on fibers to match the cellulosome system, because cellulosome has a relatively higher sensitivity to accessibility of substrate compared to free enzymes, and the generation of condensed lignin and pseudo-lignin could lower the external surface of substrate.

Abbreviations

AS	Ammonium sulfite
HT	Hydrothermal
X	Xylanase
PDI	Polydispersity index
CrI	Crystallinity index
LOI	Lateral order index
TCI	Total crystallinity index

Conflicts of interest

There are no conflicts to declare.

Acknowledgements

This research was funded by the Natural Science Foundation of China (No. 31870568), QIBEBT Research Foundation (No. QIBEBT ZZBS 201801), the Major Program of Shandong Province Natural Science Foundation (No. ZR2018ZB0208), Shandong Provincial Natural Science Foundation for Distinguished Young Scholar (China) (No. ZR2019JQ10), the "Transformational Technologies for Clean Energy and Demonstration", Strategic Priority Research Program of the Chinese Academy of Sciences (No. XDA21060201), as well as the Qingdao Source Innovation Plan (19-6-2-24-cg).

References

1 Z. Y. Zhao, J. Zuo, P.-H. Wu, H. Yan and G. Zillante, *Renewable Energy*, 2016, **89**, 144–153.
2 T. Sang, *GCB Bioenergy*, 2011, **3**, 79–90.

3 Renewable Fuels Association, *2019 Ethanol industry outlook: Powered with Renewed Energy*, 2019.
4 B. Satari, K. Karimi and R. Kumar, *Sustainable Energy Fuels*, 2019, **3**, 11–62.
5 B. Song, F. Buendia-Kandia, Y. Yu, A. Dufour and H. Wu, *Bioresour. Technol.*, 2019, **288**, 121522.
6 W. Wang, T. Q. Yuan and B. K. Cui, *Bioresources*, 2014, **9**, 3968–3976.
7 H. Xu, G. Yu, X. Mu, C. Zhang, P. DeRoussel, C. Liu, B. Li and H. Wang, *Ind. Crops Prod.*, 2015, **76**, 638–646.
8 F. P. Bouxin, J. S. David and M. C. Jarvis, *Bioresour. Technol.*, 2014, **162**, 236–242.
9 C. Liu, H. Wang, B. Li, G. Yu and X. Mu, *Biotechnol. Biofuels*, 2013, **6**, 97.
10 J. Y. Zhu, X. J. Pan, G. S. Wang and R. Gleisner, *Bioresour. Technol.*, 2009, **99**, 2411–2418.
11 G. Yu, B. Li, C. Liu, Y. Zhang, H. Wang and X. Mu, *Ind. Crops Prod.*, 2013, **50**, 750–757.
12 G. Qi, L. Xiong, L. Tian, M. Luo, X. Chen, C. Huang, H. Li and X. Chen, *Sustainable Energy Technologies and Assessments*, 2018, **29**, 12–18.
13 J. E. B. Tavares, R. M. Lukasik, T. C. B. Paiva and F. T. D. Silva, *New J. Chem.*, 2018, **42**, 4474–4484.
14 W. O. S. Doherty, P. Mousavioun and C. M. Fellows, *Ind. Crops Prod.*, 2011, **33**, 259–276.
15 L. Wei, Z. Wen, S. Hurley and L. Yan, *Appl. Biochem. Biotechnol.*, 2005, **124**, 1017–1030.
16 C. K. Nitsos, K. A. Matis and K. S. Triantafyllidis, *ChemSusChem*, 2013, **6**, 110–122.
17 Y. Zhang, X. Mu, H. Wang, B. Li and H. Peng, *J. Agric. Food Chem.*, 2014, **62**, 4661–4667.
18 S. Banerjee, S. Mudliar, R. Sen, B. Giri, D. Satpute, T. Chakrabarti and R. A. Pandey, *Biofuels, Bioprod. Biorefin.*, 2010, **4**, 77–93.
19 D. Klein-Marcuschamer, P. Oleskowicz-Popiel, B. A. Simmons and H. W. Blanch, *Biotechnol. Bioeng.*, 2012, **109**, 1083–1087.
20 Y.-J. Liu, B. Li, Y. Feng and Q. Cui, *Biotechnol. Adv.*, 2020, 107535.
21 L. R. Lynd, W. H. v. Zyl, J. E. McBride and M. Laser, *Curr. Opin. Biotechnol.*, 2005, **16**, 577–583.
22 S. Liu, Y.-J. Liu, Y. Feng, B. Li and Q. Cui, *Biotechnol. Biofuels*, 2019, **12**, 35.
23 J. Zhang, S. Liu, R. Li, W. Hong, Y. Xiao, Y. Feng, Q. Cui and Y.-J. Liu, *Biotechnol. Biofuels*, 2017, **10**, 124.
24 M. G. Resch, B. S. Donohoe, J. O. Baker, S. R. Decker, E. Bayer, G. T. Beckham and M. E. Himmel, *Energy Environ.*, 2013, **6**, 1858–1867.
25 V. A. Thomas, B. S. Donohoe, M. Li, Y. Pu, A. J. Ragauskas, R. Kumar, T. Y. Nguyen, C. M. Cai and C. E. Wyman, *Biotechnol. Biofuels*, 2017, **10**, 252.
26 T. Auxenfans, S. Buchoux, D. Larcher, G. Husson, E. Husson and C. Sarazin, *Energy Convers. Manage.*, 2014, **88**, 1094–1103.
27 H. Xu, B. Li, X. Mu, G. Yu, C. Liu, Y. Zhang and H. Wang, *Bioresour. Technol.*, 2014, **169**, 19–26.
28 X. Xie, X. Feng, S. Chi, Y. Zhang, G. Yu, C. Liu, Z. Li, B. Li and H. Peng, *Bioresource Technology Reports*, 2018, **3**, 169–176.
29 N. Kothari, E. K. Holwerda, C. M. Cai, R. Kumar and C. E. Wyman, *Biotechnol. Biofuels*, 2018, **11**, 219.
30 M. Zheng, J. Pang, R. Sun, A. Wang and T. Zhang, *ACS Catal.*, 2017, **7**, 1939–1954.
31 A. V. Heiningen, *World Pulp & Paper*, 2006, vol. 107, pp. 38–43.
32 T. K. Ghose, *Pure Appl. Chem.*, 1987, **59**, 257–268.
33 S. Chi, G. Yu, X. Zhang, Y. Zhang, C. Liu and Z. Li, *Bioresources*, 2019, **14**, 4603–4622.
34 J. Zhang, Y.-J. Liu, G.-Z. Cui and Q. Cui, *Biotechnol. Biofuels*, 2015, **8**, 36.
35 A. Sluiter, B. Hames, R. Ruiz, C. Scarlata, J. Sluiter, D. Templeton and D. Crocker, *Determination of Structural Carbohydrates and Lignin in Biomass*, National Renewable Energy Laboratory, Golden, Colo, 2012.
36 F. G. Hurtubise and H. Krassig, *Anal. Chem.*, 1960, **32**, 177–181.
37 M. Nelson and R. O'Connor, *J. Appl. Polym. Sci.*, 1964, **8**, 1325–1341.
38 L. Segal, J. J. Creely, A. E. Martin and C. M. Conrad, *Text. Res. J.*, 1959, **29**, 786–794.
39 K. K. Datta, D. Jagadeesan, C. Kulkarni, A. Kamath, R. Datta and M. Eswaramoorthy, *Angew. Chem., Int. Ed.*, 2011, **50**, 3929–3933.
40 Z. Yue, Q. Hou, W. Liu, S. Yu, X. Wang and H. Zhang, *Bioresour. Technol.*, 2019, **282**, 318–324.
41 H. Mou, E. Heikkilä and P. Fardim, *J. Agric. Food Chem.*, 2014, **62**, 3619–3625.
42 V. Reyes-Ortiz, R. A. Heins, G. Cheng, E. Y. Kim, B. C. Vernon, R. B. Elandt, P. D. Adams, K. L. Sale, M. Z. Hadi, B. A. Simmons, M. S. Kent and D. Tullman-Ercek, *Biotechnol. Biofuels*, 2013, **6**, 93.
43 S.-Y. Ding, Y.-S. Liu, Y. Zeng, M. E. Himmel, J. O. Baker and E. A. Bayer, *Science*, 2012, **338**, 1055–1060.
44 K. Linoj, C. Richard and S. Jack, *Biotechnol. Bioeng.*, 2011, **108**, 2300–2311.
45 D. Tarasov, M. Leitch and P. Fatehi, *Biotechnol. Biofuels*, 2018, **11**, 269.
46 H. Yang, Y. Xie, X. Zheng, Y. Pu, F. Huang, X. Meng, W. Wu, A. Ragauskas and L. Yao, *Bioresour. Technol.*, 2016, **207**, 361–369.
47 D. Meier, V. Zúñiga-Partida, F. Ramírez-Cano, N. C. Hahn and O. Faix, *Bioresour. Technol.*, 1994, **49**, 121–128.
48 S. Liang, J. H. Qiu, H. X. Feng, M. Z. Liu, G. H. Zhang, J. B. An, C. M. Gao and H. L. Liu, *Synth. Met.*, 2009, **159**, 1761–1766.
49 T. Q. Yuan, S. N. Sun, F. Xu and R. C. Sun, *J. Agric. Food Chem.*, 2011, **59**, 10604–10614.
50 C. Liu, C. Si, G. Wang, H. Jia and L. Ma, *Ind. Crops Prod.*, 2018, **111**, 201–211.
51 R. Lou, R. Ma, K.-T. Lin, A. Ahamed and X. Zhang, *ACS Sustainable Chem. Eng.*, 2019, **7**, 10248–10256.
52 J. Wen, B. Xue, F. Xu, R. C. Sun and A. Pinkert, *Ind. Crops Prod.*, 2013, **42**, 332–343.
53 J. S. Van Dyk and B. I. Pletschke, *Biotechnol. Adv.*, 2012, **30**, 1458–1480.

54 H. Mou, B. Li and P. Fardim, *Energy Fuels*, 2014, **28**, 4288–4293.
55 K. Daehwan, *Molecules*, 2018, **23**, 309.
56 Z. Li, J. P. O'Dwyer, V. S. Chang, C. B. Granda and M. T. Holtzapple, *Bioresour. Technol.*, 2008, **99**, 3817–3828.
57 J. Li, H. Zhang, M. Lu and L. Han, *Bioresour. Technol.*, 2019, **293**, 122016.
58 E. A. Bayer, L. J. W. Shimon, Y. Shoham and R. Lamed, *J. Struct. Biol.*, 1998, **124**, 221–234.
59 K. Yao, Q. Wu, R. An, W. Meng, M. Ding, B. Li and Y. Yuan, *AIChE J.*, 2018, **64**, 1954–1964.
60 C. Huang, X. Wu, Y. Huang, C. Lai, X. Li and Q. Yong, *Bioresour. Technol.*, 2016, **219**, 583–588.
61 J. S. Brinen, *Nord. Pulp Pap. Res. J.*, 1993, **8**, 123–129.

